Veterinary Microbiology 229 (2019) 90–99

Contents lists available at ScienceDirect

Veterinary Microbiology

journal homepage: www.elsevier.com/locate/vetmic

The bacterial and fungal microbiome of the skin of healthy dogs and dogs with atopic dermatitis and the impact of topical antimicrobial therapy, an exploratory study

Suttiwee Chermprapai[a,b,c,*], Thomas H.A. Ederveen[d,e], Femke Broere[a,c], Els M. Broens[a], Yvette M. Schlotter[c], Saskia van Schalkwijk[e], Jos Boekhorst[d,e], Sacha A.F.T. van Hijum[d,e], Victor P.M.G. Rutten[a,f]

[a] Department of Infectious Diseases and Immunology, Faculty of Veterinary Medicine, Utrecht University, Utrecht, 3584 CL, the Netherlands
[b] Department of Companion Animals Clinical Sciences, Faculty of Veterinary Medicine, Kasetsart University, Bangkok, 10900, Thailand
[c] Department of Clinical Sciences of Companion Animals, Faculty of Veterinary Medicine, Utrecht University, Utrecht, 3584 CM, the Netherlands
[d] Centre for Molecular and Biomolecular Informatics (CMBI), Radboud University Nijmegen Medical Centre, Nijmegen, 6525 GA, the Netherlands
[e] NIZO, Ede, 6718 ZB, the Netherlands
[f] Department of Veterinary Tropical Diseases, Faculty of Veterinary Science, University of Pretoria, Onderstepoort, 0110, South Africa

ARTICLE INFO

Keywords:
microbiome composition
16S
ITS
canine
atopic dermatitis
topical treatment

ABSTRACT

Canine atopic dermatitis is a genetically predisposed inflammatory and pruritic allergic skin disease that is often complicated by (secondary) bacterial and fungal (yeast) infections. High-throughput DNA sequencing was used to characterize the composition of the microbiome (bacteria and fungi) inhabiting specific sites of skin in healthy dogs and dogs with atopic dermatitis (AD) before and after topical antimicrobial treatment. Skin microbiome samples were collected from six healthy control dogs and three dogs spontaneously affected by AD by swabbing at (non-) predilection sites before, during and after treatment. Bacteria and fungi were profiled by Illumina sequencing of the 16S ribosomal RNA gene of bacteria (16S) and the internally transcribed spacer of the ribosomal gene cassette in fungi (ITS). The total cohort of dogs showed a high diversity of microbes on skin with a strong individual variability of both 16S and ITS profiles. The genera of *Staphylococcus* and *Porphyromonas* were dominantly present both on atopic and healthy skin and across all skin sites studied. In addition, bacterial and fungal alpha diversity were similar at the different skin sites. The topical antimicrobial treatment increased the diversity of bacterial and fungal compositions in course of time on both AD and healthy skin.

1. Introduction

Atopic dermatitis (AD) in dogs is a genetically predisposed inflammatory and pruritic allergic skin disease (Hensel et al. 2015). The skin microbiome may be the source of secondary infections that can influence the severity of canine AD (Santoro et al. 2015). Microbial culture-based studies showed that the most prominent bacterium on lesional skin of dogs with AD is *Staphylococcus pseudintermedius*, whereas *Malassezia pachydermatis* is the main fungal representative (Miller et al. 2013). Topical antimicrobial therapy is widely used to relieve symptoms of AD partly caused by secondary infections (Olivry et al. 2015).

Compared to human fewer studies focused on the canine skin microbiome. The relative abundance of the *Staphylococcus* genus was increased on the skin of AD dogs compared to healthy controls (Bradley et al. 2016; Bjerre et al. 2017), and lower bacterial diversity was observed at skin sites affected by AD flares in dogs (Rodrigues Hoffmann et al. 2014; Bradley et al. 2016). Likewise, fungal marker-gene sequences (ITS) revealed that the fungal diversity of lesional skin of atopic dogs was lower than that of healthy skin (Meason-Smith et al. 2015).

In dogs, specific areas of the skin are prone to be affected by AD (Favrot et al. 2010). In the present study, we aimed at characterization by high-throughput sequencing of the DNA of bacteria and fungi inhabiting the canine skin and compared the differences in microbiome composition i) at three predilection sites of canine AD (axilla, inguinal,

* Corresponding author at: Department of Companion Animals Clinical Sciences, Faculty of Veterinary Medicine, Kasetsart University, Bangkok, Thailand.
E-mail addresses: s.chermprapai@uu.nl, fvetstw@ku.ac.th (S. Chermprapai), tom.ederveen@radboudumc.nl (T.H.A. Ederveen), f.broere@uu.nl (F. Broere), e.m.broens@uu.nl (E.M. Broens), y.m.schlotter@uu.nl (Y.M. Schlotter), saskia.vanschalkwijk@nizo.com (S. van Schalkwijk), jos.boekhorst@nizo.com (J. Boekhorst), sacha.vanhijum@nizo.com (S.A.F.T. van Hijum), v.rutten@uu.nl (V.P.M.G. Rutten).

https://doi.org/10.1016/j.vetmic.2018.12.022
Received 21 September 2018; Received in revised form 14 December 2018; Accepted 17 December 2018

periocular regions) and a non-predilection site (the trunk), ii) in health and AD and iii) before, during and after topical treatment with Malaseb® shampoo containing chlorhexidine 2% and miconazole 2%, proven to be effective for prevention and control of (secondary) bacterial and yeast growth on AD skin and consequent reduction of clinical symptoms of affected dogs (Mueller et al. 2012; Olivry et al. 2015). With this exploratory study we intended to report initial descriptive data before embarking on a large survey.

2. Material and Methods

2.1. Dogs and sampling

Three atopic (AD, females, mean age 4.3 ± 4.0 SD years) and six healthy (HD, 4 females and 2 males; mean age: 4.75 ± 2.0 SD years) dogs of different breeds (Table S1) housed in the premises of the Department of Clinical Sciences of Companion Animals, Utrecht University were included. The three AD dogs were Bedlington-Beagle crossbreeds whereas the healthy dogs included three Bedlington-Beagle crossbreeds, two Beagles and one Greyhound. The AD dogs met the Favrot's diagnostic criteria for AD, and other causes of pruritus were ruled out by direct examination of the presence of fleas and flea faeces, coat brushing and skin scrapings (Hensel et al. 2015). Anti-parasitic control was achieved by monthly spot-on treatment with selamectin. Skin cytology was performed to rule out pyoderma and Malassezia dermatitis. Finally, the animals were fed an elimination diet for at least 8 weeks where food allergy was ruled out when no improvement on the diet was observed. For all nine dogs enrolled (Fig. 1), hair was clipped at three lesional sites (axillae, inguinal and periocular) and one non-lesional site (craniolateral trunk), and skin microbiome samples were collected by swabbing. A new pair of gloves was used for swabbing each sample. Sterile swabs (Isohelix DNA Buccal Swabs, Cell Projects Ltd, UK) were pre-moistened with either a sterile solution of 50 mM Tris buffer [pH 8], 1 mM EDTA, and 0.5% Tween-20 or a sterile phosphate buffered saline (PBS), for bacterial and fungal DNA isolation respectively. Swabs were placed parallel to the skin surface and rubbed back and forth for approximately 30 s. Initially, all healthy control dogs (n = 6) were enrolled in the comparison of skin microbiome compositions of different AD predilection sites. Thereafter, sex- and breed-matched healthy control (HD, n = 3) and AD (n = 3) dogs were kept untreated for four weeks and were subsequently subjected to topical antimicrobial therapy with Malaseb® shampoo (Dermcare-vet Pty Ltd, Brisbane, Australia) twice weekly for three weeks. Finally, they were again kept untreated for four weeks. Sampling was conducted as follows: t_0: before start of treatment; t_1: after three weeks of treatment; t_2: four weeks after finalizing the 3-week treatment cycle; t_f: upon occurrence of flare-up symptoms in the period between t_1 and t_2 (Fig. 1). Three AD dogs had AD lesions (erythema, lichenification, excoriations, self-induced alopecia) when the diagnosis was made, and in one of the three AD dogs AD lesions flared mainly at the inguinal area, axillae, forelimbs and hindlimbs after discontinuation of topical treatment (t_2). CADESI-03 scores of the AD dogs were between 0 and 116 at the start of the experiment and as a result of bathing the scores improved to between 0 and 33. Healthy dogs enrolled in this study did not have any skin lesions throughout the experiment. The Malaseb® shampoo was applied both on AD and healthy dogs to create similar treatment conditions for comparison of microbiome changes. All experimental procedures were approved by the Utrecht University Animal Ethic committee as required under Dutch legislation (DEC 2013.II.06.069 and DEC 2013.II.07.83)

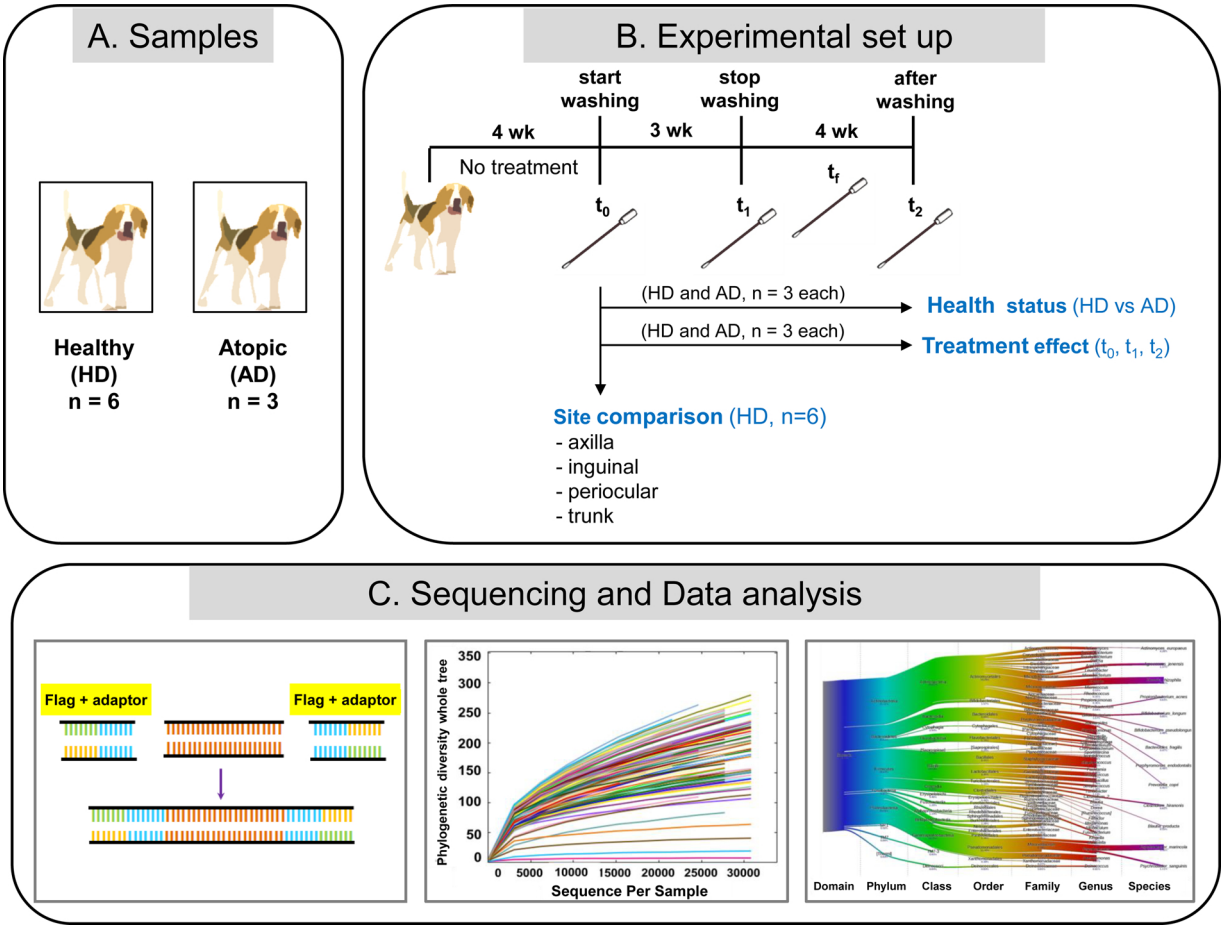

Fig. 1. Study design and timeline of topical antimicrobial treatment.

2.2. Microbial DNA extraction for marker gene sequencing

To release bacteria (16S), the cotton tips of swabs were repeatedly pressed against the wall of tubes containing 300 µl Microbead solution (MO BIO Ultraclean™ Microbial DNA Isolation Kit, MO BIO Laboratories Inc., Carlsbad, USA). Each tube was vortexed at maximum speed with the MO BIO Vortex Adapter tube holder (MO BIO Laboratories Inc., Carlsbad, USA) for 10 minutes and microbial DNA was isolated according to the manufacturer's description. The microbial DNA samples were stored at −20 °C until further use.

For analysis of fungi (ITS) the cotton tips of the swabs were individually stored in 300 µl lysis solution (MasterPure™ Yeast DNA Purification kit, Epicentre, Madison, USA) at 4 °C. Then, 20 mg/ml lysozyme (Sigma-Aldrich, St. Louis, USA) was added to the samples and incubated for 1 h while shaking (220 rpm) at 37 °C, finally, the cotton tips were removed using sterile forceps. Next, a 5 mm steel bead was added to mechanically disrupt fungal cell walls in samples using a Tissuelyser (Qiagen, Valencia, USA) for 2 min at 30 Hz. The Invitrogen PureLink Genomic DNA Kit (Invitrogen, Carlsbad, USA) was utilized for all subsequent steps. The microbial DNA samples were stored at −20 °C until further use.

2.3. Microbial DNA amplification for marker gene sequencing

Since according to a previous study in humans (Zeeuwen et al. 2012), only low amounts of microorganism DNA was found on skin as analyzed by PCR, a nested PCR was applied in the present study. In the first round of PCR, universal primers (16S: 200 nM forward primer (338 F), 5'-ACT CCT ACG GGA GGC AGC AG-3', 200 nM reverse primer (1061R), 5'CRR CAC GAG CTG ACG AC-3'; ITS: 400 nM forward primer (ITS1F), 5′-CTT GGT CAT TTA GAG GAA GTA A-3′, 400 nM reverse primer (ITS4R), 5′-TCC TCC GCT TAT TGA TAT GC-3′) were used to generally amplify the genomic DNA of the V3-V6 region of the 16S rRNA genes, and the ITS1-ITS2 region of the ITS genes, respectively. In the second round of PCR, flagged specific primers were used covering V3-V4 (16S) and ITS1-ITS2 (ITS) regions, resulting in barcoded products; for 16S: 200 nM forward primer (357 F), 5'-*TCG TCG GCA GCG TCA GAT GTG TAT AAG AGA CAG NNN NNN* **CCT ACG GGA GGC AGC AG**-3', 200 nM reverse primer (802RV2), 5'-*GTC TCG TGG GCT CGG AGA TGT GTA TAA GAG ACA G* **TA CNV GGG TAT CTA AKC C**-3'; and for ITS: 40 nM forward primer (ITS86 F), 5'- *TCG TCG GCA GCG TCA GAT GTG TAT AAG AGA CAG NNN NNN NN* **G TGA ATC ATC GAA TCT TTG AAC**-3', 40 nM reverse primer (ITS4R), 5′ *GTC TCG TGG GCT CGG AGA TGT GTA TAA GAG ACA G* **TC CTC CGC TTA TTG ATA TGC**-3′; the italicized sequence is the flag sequence, *N* is the designated barcode (adaptor) to tag each product individually and the bold sequence is the universal primer sequence. Optimal PCR conditions (50 µl reaction volume) were as follows: 5 µl of 10xKOD buffer, 5 µl of KOD dNTPs, 3 µl of KOD $MgSO_4$, forward and reverse primer, 1 µl of KOD hot start DNA polymerase (Novagen®, Osaka, Japan) and ultrapure water (Milli-Q™) for each reaction. All reactions were initiated at 95 °C for 2 min; followed by cycles of 95 °C for 20 s, 55 °C for 10 s, and 70 °C for 15 s for both 1st and 2nd rounds of PCR. Numbers of cycles for 1st and 2nd PCR were 30 and 35 for 16S respectively 25 and 25 for ITS. Each PCR product was examined for product size by electrophoresis on a 1% agarose gel and purified using a MSB Spin PCRapace kit (Invitek Inc., Carlsbad, USA) and a PureLink PCR purification kit (Invitrogen, Carlsbad, USA) for the initial and second (barcoding) PCR, respectively.

2.4. 16S and ITS marker gene sequencing

The skin microbiome compositions were determined by sequencing of the PCR products of the bacterial and fungal marker genes 16S ribosomal RNA gene (16S) and the internal transcribed spacer (ITS). For this purpose, Illumina 16S rRNA and ITS amplicon libraries were generated from the microbial DNA isolated and barcoded as described above. Aliquots of minimally 100 ng per sample and a 260/280 ratio ranging between 1.8 and 2.0 were pooled and multiplexed libraries were sequenced by BaseClear BV (Leiden, The Netherlands), on an Illumina MiSeq system with a paired-end 300 cycles protocol and indexing. The sequencing run was analyzed with the Illumina CASAVA pipeline (v1.8.3) with demultiplexing based on sample-specific barcodes. The raw sequencing data produced were processed removing the sequence reads of too low quality (only "passing filter" reads were selected) and discarding reads containing adaptor sequences or failing PhiX Control with an in-house filtering protocol. A quality assessment on the remaining reads was performed using the FASTQC quality control tool version 0.10.0.

2.5. Illumina sequence data analysis

Demultiplexed FASTQ files as provided by BaseClear were first used to generate Illumina paired-end sequence pseudoreads by PEAR (Zhang et al. 2014), using the default settings. For gene sequencing analysis, a customized Python workflow based on Quantitative Insights Into Microbial Ecology (QIIME version 1.8) (Caporaso et al. 2010) was adopted (http://qiime.org). Reads were filtered for chimeric sequences using the UCHIME algorithm version 4 (Edgar et al. 2011). Open reference OTU calling for taxonomic classification of sequencing reads was performed with USEARCH version 6.1 (Edgar, 2010) as implemented in QIIME against the Greengenes database version 13_8 for bacterial sequences (DeSantis et al. 2006), and against the UNITE database version 12_11 for fungal sequences (Koljalg et al. 2005). Hierarchical clustering of samples was performed using UPGMA with weighted UniFrac as a distance measure as implemented in QIIME. Figures resulting from these clustering analyses were generated using the interactive tree of life (iTOL) tool (Letunic and Bork, 2007). Alpha diversity metrics (phylogenetic diversity whole tree (PDWT), Chao1, Observed Species and Shannon) were calculated by bootstrapping 10 reads per sample, and taking the average over ten trials. For visualization of the differential microbiome, Cytoscape software version 3.1 3 (Shannon et al. 2003) was used together with in-house developed Python scripts for generating the appropriate input data deriving from the QIIME analysis. Fold changes in abundances of bacterial and fungal genera between healthy and AD samples of the four skin sites (the 2-log of the ratio Healthy/AD) are shown in Table 1 and Table 2 respectively, as heatmaps, created by the Excel version 2010 using the color scales of conformational formatting. Individual microbiota were ranked according to averaged relative abundances in the AD skin samples.

The average sequence read count per sample of this study was 31182 ± 5834 SD and 49064 ± 11846 SD, for 16S and ITS respectively, and likewise, the average number of operational taxonomic units (OTUs) per sample was 3053 ± 881 SD and 341 ± 158 SD. Three 16S samples were excluded from further analyses, one due to a low number of reads (44) and two others due to low OTU counts (148 and 169) (see more details in Tables S2 and S3). For an overview of the exact (16S and ITS) microbiome composition for each study sample we refer to Tables S4 and S5. Note that due to technical limitations in the resolution of 16S and ITS marker gene sequencing, OTUs calling on the level of species should be interpreted with caution.

2.6. Statistics

For the microbiome data in this manuscript, statistical significance between contrasts with regard to taxonomy abundances was tested by a non-parametric (unpaired) Mann-Whitney *U* test (MWU), uncorrected for multiple testing; unless stated otherwise. Note that in the case of uncorrected p-values, the p-value threshold that needs to be met in order to be considered significant is adapted by dividing the classic threshold of $P = 0.05$ by the number of taxa observed. Statistical tests were performed by custom, in-house Python scripts (SciPy module version 0.17.0; https://www.scipy.org/) downstream of QIIME, as

Table 1
Differential presence of bacteria (16S) in the skin microbiome on different body sites of AD and healthy skin.

Genus (Bacteria)	Axilla	Inguinal	Periocular	Trunk	Average abundance
Staphylococcus	-1.5	-3.1	-3.1	-2.1	22.09%
Psychrobacter	-2.0	-3.0	-2.7	-4.0	9.56%
Trichococcus	-2.7	-3.2	-2.7	-4.6	5.72%
Brachybacterium	-1.7	-2.4	-2.2	-2.2	3.26%
Porphyromonas	0.3	**1.6** *	0.6	-1.3	3.08%
Kocuria	0.7	1.1	1.4	0.5	2.87%
Agrococcus	-0.2	-0.5	-1.1	0.2	2.60%
Lactobacillus	-0.2	0.5	-0.7	-2.2	1.84%
Corynebacterium	1.0	**1.5** *	0.2	2.0	1.51%
Turicibacter	0.7	1.3	**1.1** *	0.2	1.19%
Dietzia	0.5	**1.6** *	1.2	1.0	0.91%
Facklamia	-0.2	0.0	0.5	-0.7	0.86%
Pseudomonas	2.8	**5.3** *	2.9	0.0	0.83%
Microbacterium	**1.5** *	**1.9** *	**1.9** *	0.7	0.69%
Leucobacter	-0.4	-1.0	0.1	0.1	0.68%
Actinomyces	1.6	**1.9** *	**1.5** *	1.1	0.67%
Clostridium	1.1	2.7	0.9	1.2	0.64%
Chryseobacterium	0.9	1.2	0.6	-0.1	0.60%
Moraxella	1.7	1.2	0.4	-0.8	0.60%
Prevotella	0.4	0.0	-0.3	-1.6	0.60%

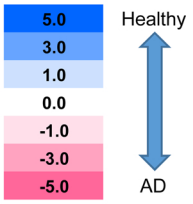

Listed are the 20 (out of 496) on average most abundant bacterial genera of atopic dermatitis dogs from three predilection sites: axilla, inguinal region and periocular, and one non-predilection site: trunk. Ranking is based on the averaged relative abundances of bacteria of the four skin sample sites in the three AD dogs. The heatmap presents the fold changes in abundance (the 2-log of the ratio Healthy/AD): 1 means two times more abundant in healthy samples, -1 means two times more abundant in AD samples, 0 means no change, etc. Significant differences (* $P < 0.05$) in relative abundance of genera in AD compared to healthy skin at the same sampling site were determined by MWU. A Bonferroni-corrected P value threshold for significance is the genus-level P value divided by the number of total genera identified, $0.05/496 = P < 1.0*10^{-4}$. For abundances of the remaining genera and other taxon levels, see Table S4.

described above. Principal component analysis (PCA) as well as multivariate Redundancy Analysis (RDA) were done using Canoco 5.04 (Cajo et al., 2012) using default settings of the analysis type 'Unconstrained' or 'Constrained', respectively. Canoco reported variance explained by particular variables (e.g. breed and site) by applying said variables as single supplementary variables in a PCA analysis. Relative abundance values for taxa were used as response data, and for RDA, the sample classes as explanatory variables. RDA calculates P values by permuting the sample classes. Significances mentioned in figures are as follows: n.s. (not significant), * $P < 0.05$.

2.7. Accession numbers

The raw, unprocessed 16S rRNA and ITS marker gene Illumina sequence reads are publicly available for download at the European Nucleotide Archive (ENA) database (Leinonen et al. 2011) under study accession number: PRJEB20808 (http://www.ebi.ac.uk/ena/data/view/PRJEB20808) or secondary accession number: ERP022994 (http://www.ebi.ac.uk/ena/data/view/ERP022994). The sequencing data are available in FASTQ-format, includissng corresponding metadata for each sample. For additional information on sample characteristics we refer to Table S1.

3. Results

3.1. Canine skin microbiome: general aspects

3.1.1. Study demographics and overview of canine skin microbiome

Bacterial (16S) and fungal (ITS) microbiome compositions of both healthy and AD dog skin at four different sites (axilla, inguinal, periocular and trunk) and at three different time-points (before, during and after Malaseb® treatment) were assessed by a PCA at the genus-level. PCA showed clear separation (variance) between sample groups (Fig. 2). Most notably, distances between sample sites were less than those between health and AD states or between time-points around treatment (Malaseb® treatment effect) for both 16S and ITS, indicating that there is more overlap between microbiome composition and abundance between different skin niches than between health states and between stages (i.e. effect) of treatment.

3.1.2. Comparison of microbiome composition on different (non-) predilection skin sites within healthy or AD dogs

In RDA, the bacterial and fungal skin microbiome composition on genus-level in healthy dogs did not differ significantly between skin niches defined as AD predilection (axilla, inguinal and periocular) or non-predilection (trunk) sites, for 16S ($P = 0.2$) nor ITS ($P = 0.3$). Accordingly, a clear clustering of samples collected from similar body sites based on microbiome composition was not observed (Figs. S1-S4). However, the samples collected from different skin sites of the same individual did show a certain degree of variation in microbial composition (both 16S and ITS) but samples from the same breed were at relatively close distance. For 16S, 47.0% of the variation was explained by individual differences, 30.7% by breed and 11.6% by sampling site (Fig. S5A). For ITS, these figures were 40.0%, 28.0% and 10.8% respectively (Fig. S5B). Notably, separation based on breed is more convincing for ITS than for 16S, supported by (beta diversity) clustering of samples based on full community composition (Figs. S1-S2).

3.2. Comparison of skin microbiome composition between healthy and AD skin

3.2.1. Alpha diversity

The differences in alpha diversity of bacteria (Fig. 3A) nor fungi (Fig. 3B) were statistically significant between corresponding AD and

Table 2
Differential presence of fungi (ITS) in the skin microbiome on different body sites of AD and healthy skin.

Genus (Fungi)	Axilla	Inguinal	Periocular	Trunk	Average abundance
"Unidentified#01"	0.5	-0.3	-0.3	0.3	15.87%
Blumeria	**-1.7***	**-1.7***	-1.5	**-1.8***	8.59%
"Unidentified#12"	-0.1	0.0	-0.4	0.6	7.72%
Epicoccum	-0.3	0.2	-0.2	0.4	3.83%
Fusarium	-0.2	-0.7	-2.1	0.6	2.48%
Cryptococcus	-0.9	-0.3	**-2.5***	-0.3	1.43%
Pilidium	-2.4	0.0	0.0	-1.7	1.00%
Sporobolomyces	0.8	**2.2***	0.1	**-1.8***	0.80%
Rhodotorula	**1.8***	0.3	**1.1***	0.0	0.69%
Gibberella	-0.1	1.9	**-2.3***	3.2	0.51%
"Unidentified#13"	1.5	-2.0	**0.0***	2.8	0.49%
"Unidentified#6"	**-4.0***	0.1	-5.7	-0.6	0.33%
Ramularia	0.6	**5.4***	0.0	0.4	0.27%
Alternaria	3.5	-0.6	-1.1	-2.0	0.24%
Cystofilobasidium	-2.3	-2.9	0.2	0.0	0.17%
"Unidentified#45"	**0.0***	-1.4	0.0	-1.1	0.15%
"Unidentified#23"	0.0	-5.4	0.0	0.0	0.13%
Dinemasporium	-2.0	-1.6	2.0	1.8	0.13%
Microdochium	1.0	3.6	-1.6	0.4	0.13%
Claviceps	0.0	2.3	0.0	-1.8	0.12%

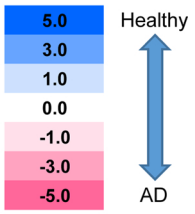

Listed are the 20 (out of 314) on average most abundant fungal genera of atopic dermatitis dogs from three predilection sites: axilla, inguinal region and periocular, and one non-predilection site: trunk. Ranking is based on the averaged relative abundances of fungi of the four skin sample sites in the three AD dogs. The heatmap presents the fold changes in abundance (the 2-log of the ratio Healthy/AD): 1 means two times more abundant in healthy samples, -1 means two times more abundant in AD samples, 0 means no change, etc. Note that "*Unidentified*" genera represent known classifiable taxa but currently without assigned nomenclature. Significant differences (* $P < 0.05$) in relative abundance of genera in AD compared to healthy skin at the same sampling site were determined by MWU. A Bonferroni-corrected P value threshold for significance is the genus-level P value divided by the number of total genera identified, $0.05/314 = P < 1.6*10^{-4}$. For abundances of the remaining genera and other taxon levels, see Table S5.

healthy skin sites; nevertheless, alpha diversity tended to be lower in AD skin at most sites studied (Fig. 3**A–B**).

3.2.2. Differential composition of the microbiome on different body sites between AD and healthy skin

Based on RDA, differences in genera contributing to the microbiome composition of both 16S and ITS associated to disease status (AD versus healthy) were not statistically significant (data not shown). The predominant genera based on body sites and health states are shown in Table 1 (16S) and Table 2 (ITS).

In both AD and healthy dog skin, the bacterial microbiome composition differed only slightly among skin sites studied (Table 1). The, on average (across all skin sites), most abundant bacteria observed in AD skin were *Staphylococcus*, *Psychrobacter*, *Trichococcus*, *Brachybacterium* and *Porphyromonas*. These genera were also present on healthy skin but varied in the relative abundance. The most dominant bacterial (genus-level) taxa shared between all four body sites in healthy skin are *Pseudomonas* (5.61% ± 1.96% SEM), *Kocuria* (5.29% ± 0.62%), *Porphyromonas* (4.31% ± 1.52%), *Staphylococcus* (3.65% ± 0.72%) and *Corynebacterium* (3.31% ± 1.08%) (Table S4). Differences were observed in the order of the top abundant taxa among the sample sites of dogs with AD (Table 1). *Staphylococcus* was always more abundant in AD skin than in controls at the same sites (axilla: 14.46% versus 5.02%; inguinal 36.50% versus 4.26%; periocular 30.46% versus 3.66%; trunk 6.95% versus 1.66%) (Fig. S6, t_0 results), although this did not reach statistical significances. In samples of lesional sites of AD dogs during flare-up the presence of *Staphylococcus* was the most abundant among the bacterial microbiome community (21.74 ± 8.29% SEM). Interestingly, the relative abundances of the lowly dominant *Microbacterium* were significantly lower at each of the three predilection sites in AD dogs as compared to those in healthy ones (Table 1). In contrast, for none of the 496 bacterial genera significant differences in relative abundance were found between AD and healthy trunk skin, considered to be a non-predilection site.

The most abundant fungal genera, found on the healthy skin across all sites studied were "*Unidentified#01*", a known classifiable fungal taxon but currently without assigned nomenclature, (17.28% ± 3.26% SEM), "*Unidentified#12*" (7.97% ± 1.01%), *Epicoccum* (4.02% ± 0.63%), *Blumeria* (2.68% ± 0.32%) and *Ramularia* (2.66% ± 2.31%). Like in healthy skin, "*Unidentified#01*" was the most abundant at every AD skin site studied (Table 2), and this genus was also the most dominant taxon of fungi presenting during flare-up of AD (15.46% ± 1.79% SEM).

The largest differences in relative abundances at fungal genus-level between AD and healthy skin were those observed for *Blumeria*. These were statistically significant increases at axilla, inguinal and trunk of AD skin (Table 2 and Fig. S7, t_0).

3.3. Topical antimicrobial treatment with Malaseb® shampoo

3.3.1. The effect of treatment on the diversity of the microbiome on canine skin

Bacterial and fungal diversities on healthy as well as AD skin, did not differ significantly at the three different time-points, before, during and after treatment (see Fig. S8). Interestingly, however, the trend observed in the bacterial diversity in AD skin was an initial increase from t_0 (start of treatment after at least 4 weeks without intervention) to t_1 (termination of treatment) and a subsequent decrease to the level of t_0 in the four weeks towards t_2. The fungal diversity at both AD and

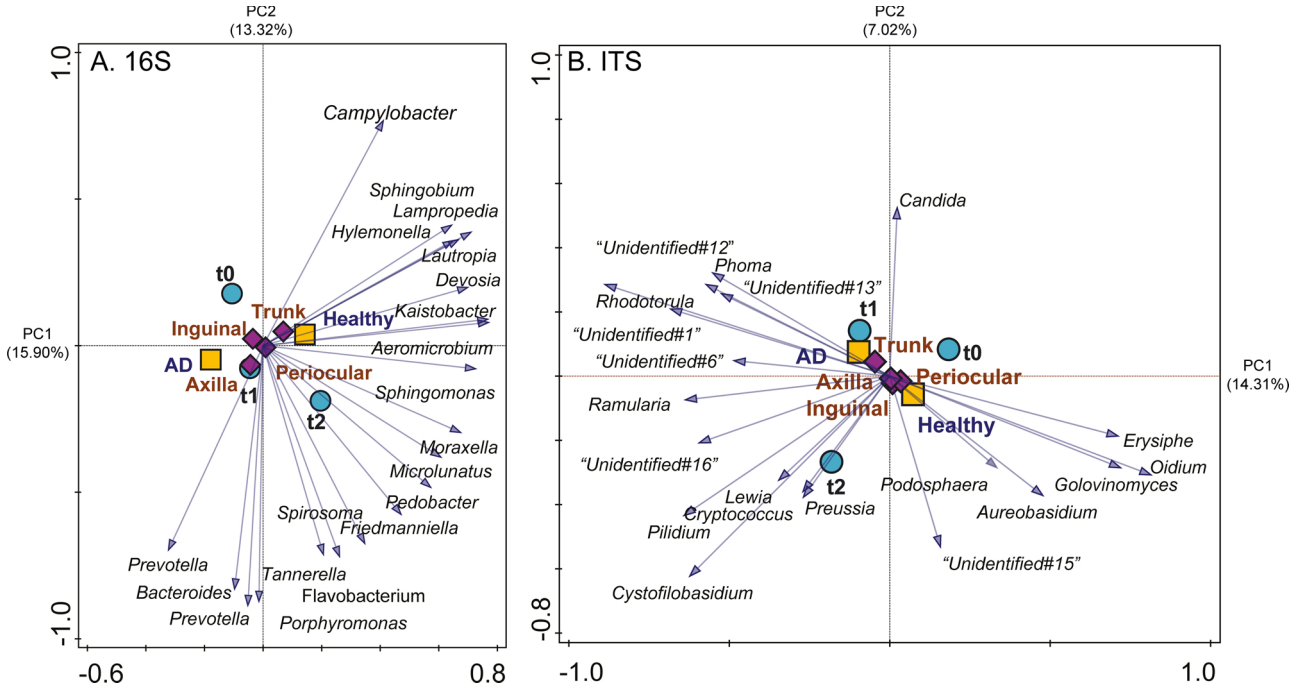

Fig. 2. Bacterial and fungal genus-level compositions of all study samples indicate a higher microbial similarity between sample sites than between health states or treatment stages. These representations of a principal component analysis (PCA) of both 16S (**A**) and ITS (**B**) datasets reflect the distances between study samples based on genus-level microbial composition and abundances for each sample. Centroids representing samples of the same sample group are shown as colored symbols accompanied by their respective labels (◆ skin site: axilla, inguinal, periocular, trunk; ■ health status: AD, healthy; ● time-point during Malaseb® treatment: t_0 before washing, t_1 after three weeks of washing, t_2 four weeks after termination of washing). The blue arrows point to the genera (names shown in italics) explaining compositional differences between the samples. Note that "*Unidentified*" genera represent known classifiable taxa but currently without assigned nomenclature.

healthy skin decreased towards t_1 and had increased at t_2, close to that at t_0. In addition, although not statistically significant, a lower diversity was observed in AD skin as compared to healthy skin at all time-points.

3.3.2. The effect of topical treatment on 16S and ITS microbiome composition

Topical treatment of dog skin caused changes in 16S microbiome composition (AD and healthy skin data combined) in course of time. A clear separation between time-points, as a result of treatment, (3 different colored ovals) was seen in axilla (Fig. 4**A**; $P = 0.026$), inguinal (Fig. 4**B**; $P = 0.032$), periocular region (Fig. 4**C**; $P = 0.004$) and trunk (Fig. 4**D**; $P = 0.028$).

Likewise, the ITS microbiome composition (AD and healthy skin data combined) at all sample sites changed significantly in course of time (axilla and trunk, Fig. 5**A** and **D** at $P = 0.001$; inguinal, Fig. 5**B** at $P = 0.019$; periocular, Fig. 5**C** at $P = 0.049$).

Hence, both the differences in bacterial (16S, Fig. 4) and fungal (ITS, Fig. 5) skin composition in course of time (treatment effect) were statistically significant if samples were not stratified on health condition (i.e. analysis irrespective of AD).

3.3.3. The most notable changes as a result of topical treatment

The most notable changes in the microbiome, as a result of treatment were observed in the genus *Epicoccum (*ITS) (Fig. S9). In AD dogs, the genus of *Blumeria* revealed the largest changes in the relative abundance determined by time-points of sampling (treatment effect) in comparison to the other fungal genera identified (Fig. S7). Its abundance was high in untreated AD skin (t_0), decreased after treatment (t_1) and remained low until four weeks after treatment withdrawal (t_2) (Fig. S7; for axilla, trunk and inguinal). The abundance of *Blumeria* on healthy skin was constantly low at all time-points and clearly lower than that on AD skin.

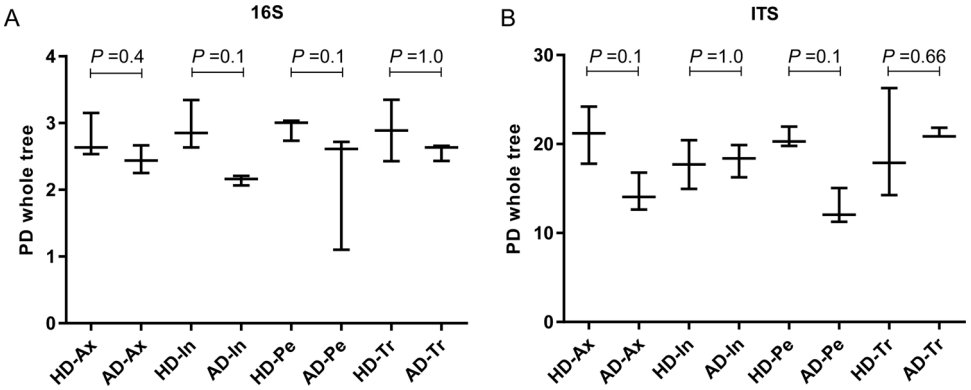

Fig. 3. Phylogenetic Diversity Whole tree (PDWT) analysis of 16S and ITS data. The diversity analyzed by PDWT of 16S (**A**) and ITS (**B**) microbiome profiles observed in atopic dermatitis (AD) and healthy (HD) skin at the four sites studied (Ax: axilla, In: inguinal, Pe: periocular, Tr: trunk).

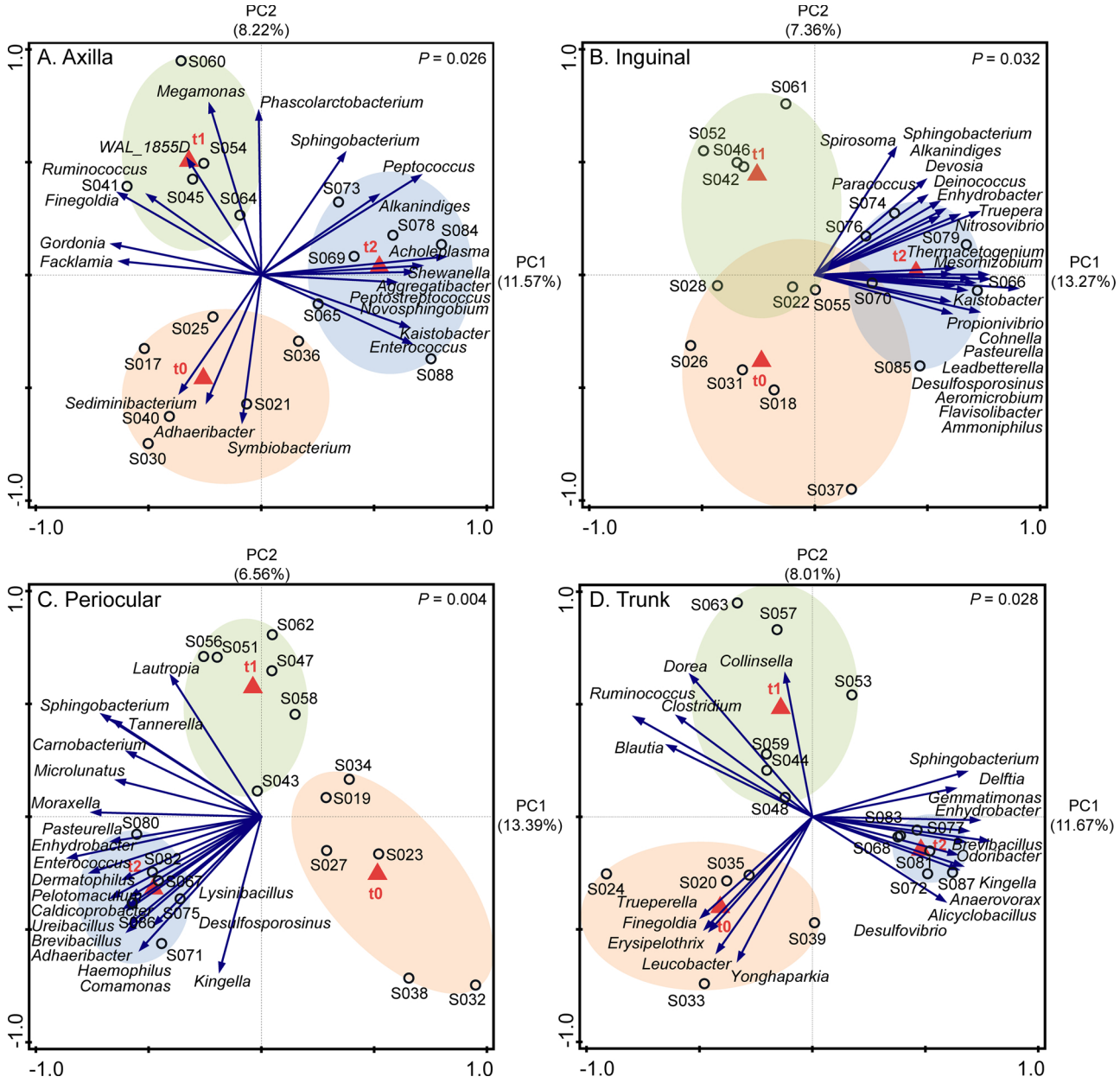

Fig. 4. Treatment effect on 16S profiles at different body sites. The16S microbiome composition associated to Malaseb® treatment at axilla (**A**), inguinal (**B**), periocular (**C**) and trunk (**D**), based on all data (irrespective of health status) visualized in a redundancy analysis (RDA) plot (Treatment was used as explanatory variable, corrected for Health Condition). Each small open circle represents the skin genus-level composition of one sample. The red triangles are the centroids of the sample groups for each time point t_0, t_1 and t_2, whereas the colored sample overlays represent the sample clusters per time-point; orange: t_0, green: t_1 and blue: t_2). Blue arrows: taxa that most contribute to the separation on samples in the respective directions. Significance level at $P < 0.05$.

4. Discussion

This study aimed to investigate both the bacterial (16S) and fungal (ITS) skin microbiome compositions, both in different individuals, at different predilection sites and with respect to the health status (AD versus healthy). Furthermore, changes were recorded in the microbiome composition after topical treatment with Malaseb® shampoo, a common choice of treatment known to reduce the clinical severity of AD most likely partly due to (secondary) infection.

Analysis of the skin 16S and ITS microbiome composition in the present cohort of dogs revealed a strong inter-dog variability (individual), whereas breed effects were considerable, but less. In samples collected from different body sites both from AD and healthy dogs, no significant differences in microbiome composition (both 16S and ITS) were found. This confirms findings of another study on fungal composition of canine skin (Meason-Smith et al. 2015). In contrast, on human skin the microbiome composition was shown to differ depending on body sites (Grice et al. 2009; Findley et al. 2013), however comparison of microbiome compositions between human and canine skin is complicated due to strongly differing microbiomes. Moreover in dogs alpha diversity of skin microbiome was considerably higher than that in humans (Zeeuwen et al. 2012; Takemoto et al. 2015).

Comparing AD and healthy skin microbiome profiles, no significant differences in the alpha diversity were found, only a trend of reduced 16S and ITS diversity in AD compared to control skin. A similar trend was reported in other canine studies (Rodrigues Hoffmann et al. 2014; Meason-Smith et al. 2015; Bradley et al. 2016). The topical treatment increases the diversity of bacteria, but the opposite effect was observed for fungal diversity. Those non-significant changes, that may be explained by difference between broad antibacterial and antifungal effects

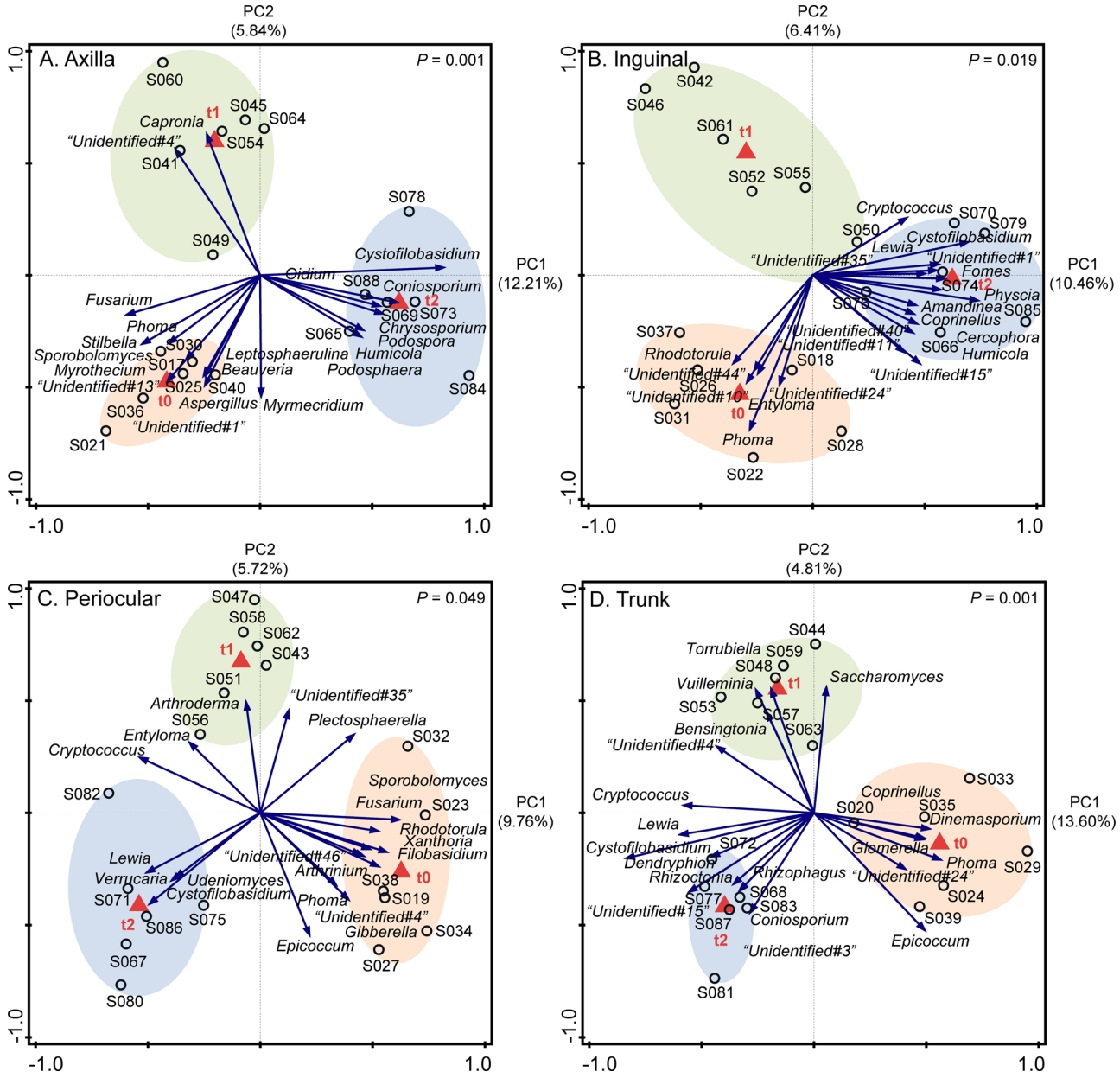

Fig. 5. Treatment effect on ITS profiles at different body sites. The ITS microbiome composition associated to Malaseb® treatment at axilla (**A**), inguinal (**B**), periocular (**C**) and trunk (**D**), based on all data (irrespective of health status) visualized in a redundancy analysis (RDA) plot (Treatment was used as explanatory variable, corrected for Health Condition). Each small open circle represents the skin genus-level composition of one sample. The red triangles are the centroids of the sample groups for each time point t_0, t_1 and t_2, whereas the colored sample overlays represent the sample clusters per time-point; orange: t_0, green: t_1 and blue: t_2). Blue arrows: taxa that most contribute to the separation on samples in the respective directions. Significant level at $P < 0.05$.

of the shampoo, and in potential differences in population dynamics amongst bacteria and fungi after treatment, need to be confirmed in larger studies. However, treatment with an antimicrobial shampoo, known to successfully alleviate clinic symptoms of AD, significantly changed both 16S and ITS profiles of the microbiome in course of time and at every site studied but irrespective of AD skin status. Only the genus, *Blumeria* (ITS), showed considerable changes in relative abundance determined by both health status and treatment effect. Whether these changes are affected by the atopic dermatitis directly or the associated inflammation, or by both, is unclear. The significant increase of this genus ($P < 0.05$; uncorrected) observed on AD as compared to healthy skin in the present study, even though it contrasts findings in an earlier study of fungi on canine skin (Meason-Smith et al. 2015), warrants further studies on the relationship between skin health status and *Blumeria*.

In the present study, the bacterial genera *Staphylococcus* and *Porphyromonas* were dominantly present in both AD and healthy skin. The finding of *Staphylococcus* as the predominant colonizer of the 16S profile on AD skin is consistent with many other studies in canine (Rodrigues Hoffmann et al. 2014; Bradley et al. 2016), feline (Older et al. 2017) and human skin (Grice et al. 2009; Kong et al. 2012). Staphylococci are common commensals on the canine skin (Weese, 2013). *Porphyromonas*, commonly found in the canine oral cavity (Falagas and Siakavellas, 2000), may have been transferred to skin by licking, presumably more frequently in AD dogs due to itch. Other genera present on healthy skin, *Kocuria*, *Pseudomonas* and *Corynebacterium* are common to dog skin (Weese, 2013; Rodrigues Hoffmann et al. 2014). The abundance of the low abundant *Microbacterium* was significantly different ($P < 0.05$; uncorrected) when compared between AD and control skin on all predilection sites but not

on the trunk (non-predilection). The observed significant differences in the lowly abundant genera might be due to the reduced alpha diversity observed in the AD skin microbiome.

The most abundant fungal genera on both canine AD and healthy were "*Unidentified#01*", "*Unidentified#12*", *Blumeria* and *Epicoccum*. Due to technical limitation of ITS marker gene analyses, "*Unidentified#01*" can only be qualified as not belonging to the phyla *Ascomycota* or *Basidiomycota,* and "*Unidentified#12*" as belonging to the phylum *Ascomycota. Malassezia* one of the most dominant yeasts (fungi) reported on canine skin (Meason-Smith et al. 2015), when it comes to identification of the microbiota composition by culture, was hardly detected in the present ITS marker gene analysis, that has shown to readily detect *Malassezia* if used as a positive control. Apparently, the skins of dogs in our study are virtually devoid of the *Malassezia* genus (presence of 0.02% on average). The ITS sequencing data was scrutinized by aligning the raw sequencing data by hand to the representative *Malassezia* ITS genus sequence to ensure that *Malassezia* reads were indeed not missed even in the raw sequencing data (results not shown). The apparent discrepancy between *Malassezia* presence as described in the literature and our study may be partially explained by housing condition and/or a small sample size of our study. The other limitations of our study include varied CADESI scores, mild secondary infections and low breed diversity.

Obviously additional factors giving rise to abnormalities as reflected in AD such as skin barrier function, immune responses, genetic background, etc., may affect the microbiome composition (Santoro et al. 2015; Chermprapai et al. 2018). Differences in skin health caused by AD might alter its capacity to deal with changes in microbiome composition (Santoro et al. 2015; Bradley et al. 2016). Interaction between microbiome and AD is likely to be a two-way street where microbiome and disease factors influence each other (Santoro et al. 2015; Bjerre et al. 2017). The predominant taxa and multiple factors potentially disturbing skin integrity in AD-related circumstances should be further investigated in a larger study.

5. Conclusion

Taken together, this study shows that the variation in microbiome composition of canine skin is likely to be dependent on individuality, and to a lesser extent is determined by skin site, health status or treatment effect. However, in some specific taxa significant differences could be observed by disease or treatment effect that need to be further investigated.

6. Declarations of interest

None

Acknowledgements

We would like to thank Patrick Zeeuwen for support in DNA sampling, isolation and amplification. This work was supported by a scholarship from the Faculty of Veterinary Medicine, Kasetsart University, Bangkok, Thailand; and a ZonMw/NWO-ALW grant "Enabling Technologies" project number 40-43500-98-091. The funding sources had no involvement in study design; the collection, analysis and interpretation of data; in the writing of the report; and in the decision to submit the article for publication.

Appendix A. Supplementary data

Supplementary material related to this article can be found, in the online version, at doi:https://doi.org/10.1016/j.vetmic.2018.12.022.

References

Bjerre, R.D., Bandier, J., Skov, L., Engstrand, L., Johansen, J.D., 2017. The role of the skin microbiome in atopic dermatitis: a systematic review. Br. J. Dermatol. 177, 1272–1278.
Bradley, C.W., Morris, D.O., Rankin, S.C., Cain, C.L., Misic, A.M., Houser, T., Mauldin, E.A., Grice, E.A., 2016. Longitudinal Evaluation of the Skin Microbiome and Association with Microenvironment and Treatment in Canine Atopic Dermatitis. J. Invest. Dermatol. 136, 1182–1190.
Cajo, J., ter Braak, F., Smilauer, Petr, 2012. Canoco Reference Manual and User's Guide: Software for Ordination (version 5.0).
Caporaso, J.G., Kuczynski, J., Stombaugh, J., Bittinger, K., Bushman, F.D., Costello, E.K., Fierer, N., Pena, A.G., Goodrich, J.K., Gordon, J.I., Huttley, G.A., Kelley, S.T., Knights, D., Koenig, J.E., Ley, R.E., Lozupone, C.A., McDonald, D., Muegge, B.D., Pirrung, M., Reeder, J., Sevinsky, J.R., Turnbaugh, P.J., Walters, W.A., Widmann, J., Yatsunenko, T., Zaneveld, J., Knight, R., 2010. QIIME allows analysis of high-throughput community sequencing data. Nat. Methods 7, 335–336.
Chermprapai, S., Broere, F., Gooris, G., Schlotter, Y.M., Rutten, V.P.M.G., Bouwstra, J.A., 2018. Altered lipid properties of the stratum corneum in Canine Atopic Dermatitis. Biochim. Biophys. Acta 1860, 526–533.
DeSantis, T.Z., Hugenholtz, P., Larsen, N., Rojas, M., Brodie, E.L., Keller, K., Huber, T., Dalevi, D., Hu, P., Andersen, G.L., 2006. Greengenes, a chimera-checked 16S rRNA gene database and workbench compatible with ARB. Appl. Environ. Microbiol. 72, 5069–5072.
Edgar, R.C., 2010. Search and clustering orders of magnitude faster than BLAST. Bioinformatics 26, 2460–2461.
Edgar, R.C., Haas, B.J., Clemente, J.C., Quince, C., Knight, R., 2011. UCHIME improves sensitivity and speed of chimera detection. Bioinformatics 27, 2194–2200.
Falagas, M.E., Siakavellas, E., 2000. Bacteroides, Prevotella, and Porphyromonas species: a review of antibiotic resistance and therapeutic options. Int. J. Antimicrob. Agents 15, 1–9.
Favrot, C., Steffan, J., Seewald, W., Picco, F., 2010. A prospective study on the clinical features of chronic canine atopic dermatitis and its diagnosis. Vet. Dermatol. 21, 23–31.
Findley, K., Oh, J., Yang, J., Conlan, S., Deming, C., Meyer, J.A., Schoenfeld, D., Nomicos, E., Park, M., NIH Intramural Sequencing Center Comparative Sequencing Program, Kong, H.H., Segre, J.A., 2013. Topographic diversity of fungal and bacterial communities in human skin. Nature 498, 367–370.
Grice, E.A., Kong, H.H., Conlan, S., Deming, C.B., Davis, J., Young, A.C., NISC Comparative Sequencing Program, Bouffard, G.G., Blakesley, R.W., Murray, P.R., Green, E.D., Turner, M.L., Segre, J.A., 2009. Topographical and temporal diversity of the human skin microbiome. Science 324, 1190–1192.
Hensel, P., Santoro, D., Favrot, C., Hill, P., Griffin, C., 2015. Canine atopic dermatitis: detailed guidelines for diagnosis and allergen identification. BMC Vet. Res. 11 196-015-0515-5.
Koljalg, U., Larsson, K.H., Abarenkov, K., Nilsson, R.H., Alexander, I.J., Eberhardt, U., Erland, S., Hoiland, K., Kjoller, R., Larsson, E., Pennanen, T., Sen, R., Taylor, A.F., Tedersoo, L., Vralstad, T., Ursing, B.M., 2005. UNITE: a database providing web-based methods for the molecular identification of ectomycorrhizal fungi. New Phytol. 166, 1063–1068.
Kong, H.H., Oh, J., Deming, C., Conlan, S., Grice, E.A., Beatson, M.A., Nomicos, E., Polley, E.C., Komarow, H.D., NISC Comparative Sequence Program, Murray, P.R., Turner, M.L., Segre, J.A., 2012. Temporal shifts in the skin microbiome associated with disease flares and treatment in children with atopic dermatitis. Genome Res. 22, 850–859.
Leinonen, R., Akhtar, R., Birney, E., Bower, L., Cerdeno-Tarraga, A., Cheng, Y., Cleland, I., Faruque, N., Goodgame, N., Gibson, R., Hoad, G., Jang, M., Pakseresht, N., Plaister, S., Radhakrishnan, R., Reddy, K., Sobhany, S., Ten Hoopen, P., Vaughan, R., Zalunin, V., Cochrane, G., 2011. The European Nucleotide Archive. Nucleic Acids Res. 39, D28–31.
Letunic, I., Bork, P., 2007. Interactive Tree Of Life (iTOL): an online tool for phylogenetic tree display and annotation. Bioinformatics 23, 127–128.
Meason-Smith, C., Diesel, A., Patterson, A.P., Older, C.E., Mansell, J.M., Suchodolski, J.S., Rodrigues Hoffmann, A., 2015. What is living on your dog's skin? Characterization of the canine cutaneous mycobiota and fungal dysbiosis in canine allergic dermatitis. FEMS Microbiol. Ecol. 91https://doi.org/10.1093/femsec/fiv139. Epub 2015 Nov 4.
Miller, W.H., Griffin, C.E., Campbell, K.L., Muller, G.H., 2013. Muller and Kirk's Small Animal Dermatology7: Muller and Kirk's Small Animal Dermatology. Elsevier/Mosby.
Mueller, R.S., Bergvall, K., Bensignor, E., Bond, R., 2012. A review of topical therapy for skin infections with bacteria and yeast. Vet. Dermatol. 23 (330-41), e62.
Older, C.E., Diesel, A., Patterson, A.P., Meason-Smith, C., Johnson, T.J., Mansell, J., Suchodolski, J.S., Rodrigues Hoffmann, A., 2017. The feline skin microbiota: The bacteria inhabiting the skin of healthy and allergic cats. PLoS One 12, e0178555.
Olivry, T., DeBoer, D.J., Favrot, C., Jackson, H.A., Mueller, R.S., Nuttall, T., Prelaud, P., International Committee on Allergic Diseases of Animals, 2015. Treatment of canine atopic dermatitis: 2015 updated guidelines from the International Committee on Allergic Diseases of Animals (ICADA). BMC Vet. Res. 11 210-015-0514-6.
Rodrigues Hoffmann, A., Patterson, A.P., Diesel, A., Lawhon, S.D., Ly, H.J., Elkins Stephenson, C., Mansell, J., Steiner, J.M., Dowd, S.E., Olivry, T., Suchodolski, J.S., 2014. The skin microbiome in healthy and allergic dogs. PLoS One 9, e83197.
Santoro, D., Marsella, R., Pucheu-Haston, C.M., Eisenschenk, M.N., Nuttall, T., Bizikova, P., 2015. Review: Pathogenesis of canine atopic dermatitis: skin barrier and host-micro-organism interaction. Vet. Dermatol. 26, 84–e25.
Shannon, P., Markiel, A., Ozier, O., Baliga, N.S., Wang, J.T., Ramage, D., Amin, N.,

Schwikowski, B., Ideker, T., 2003. Cytoscape: a software environment for integrated models of biomolecular interaction networks. Genome Res. 13, 2498–2504.
Takemoto, A., Cho, O., Morohoshi, Y., Sugita, T., Muto, M., 2015. Molecular characterization of the skin fungal microbiome in patients with psoriasis. J. Dermatol. 42, 166–170.
Weese, J.S., 2013. The canine and feline skin microbiome in health and disease. Vet. Dermatol. 24, 137–145 e31.
Zeeuwen, P.L., Boekhorst, J., van den Bogaard, E.H., de Koning, H.D., van de Kerkhof, P.M., Saulnier, D.M., van II, S., van Hijum, S.A., Kleerebezem, M., Schalkwijk, J., Timmerman, H.M., 2012. Microbiome dynamics of human epidermis following skin barrier disruption. Genome Biol. 13, R101.
Zhang, J., Kobert, K., Flouri, T., Stamatakis, A., 2014. PEAR: a fast and accurate Illumina Paired-End reAd mergeR. Bioinformatics 30, 614–620.